

## Antibacterial Activity of Chitosan Extracted from *Mucor rouxii*

Mohammed A. Abbas<sup>1</sup> and Rana H.H. Al-Shammari<sup>2</sup>

<sup>1</sup>Researcher (Master Student), Department of Biology, Collage of Science, Mustansiriyah University, Baghdad, IRAQ.

<sup>2</sup>Assistant Professor, Department of Biology, Collage of Science, Mustansiriyah University, Baghdad, IRAQ.

<sup>2</sup>Corresponding Author: dr.rana@uomustansiriya.edu.iq



www.jrasb.com || Vol. 1 No. 5 (2022): December Issue

Received: 06-11-2022

Revised: 27-11-2022

Accepted: 07-12-2022

### ABSTRACT

*Mucor rouxii* was selected due to the high biomass production and significant quantities of chitosan in its cell walls. *M. rouxii* cultured in Potato dextrose Broth for 96 hrs. at 30 C° in a shaking incubator at 150 rpm and 5.5 pH, then the fungal mycelial were dried, grounded and weighted. Mycelial dry weight in total was 68.8g with a yield of  $1.72 \pm 0.25$  g/500ml, chitosan was extracted using the classic chemical method followed by precipitation of chitosan by using sodium hydroxide. chitosan yield was 2.13%, The degree of deacetylation of chitosan extracted from *M. rouxii* was 82.22% with low Molecular weight 63.67 kDa. The Antimicrobial properties of extracted chitosan was studied on four pathogenic bacteria by MIC method the most resistant strains which were *S. aureus*, whereas the most vulnerable strains were *A. baumannii* and *E. coli*. to produce natural chitosan and replace old sources (crustaceans). The observed antimicrobial properties also indicate an acceptable effect of chitosan on some strains that needs further study.

**Keywords-** Antibacterial, chitosan, *mucor rouxii*.

## I. INTRODUCTION

Chitin is a polymer made from units N-acetyl-D- Glucosamine which is the most abundant polymer after cellulose It is obtained by the distillation of chitin under alkaline conditions [1]. The unique properties of chitosan make it widely in various industries, including cosmetic, Food additives, antimicrobial activity and water purification[2,3]. Chitosan commercially obtained from waste from Crustaceans. But it's limited for seasonal production and specific places also extraction method in addition to complexity and the high cost has many negative environmental impacts also due to the use of severely acidic conditions in the extraction process [4]. Potential benefits of use fungi as sources of chitosan because rapid grown harvesting and handling in simple culture media, Easy product quality control and ease of extraction, fungi have a high and wide ecological distribution [5]. In addition, fungi have more identical compounds and fewer mineral easy controlling the effective parameters in cultivation the amount of chitosan Controlled also the effect of time on chitosan

yield and other growth factors study [6]. Therefore, according to the mentioned advantages *Mucor* chosen for fungal chitosan production is investigated and finally the antimicrobial properties of extracted chitosan is examined.

## II. MATERIALS AND METHODS

### *Rhizopus* isolation, identification and biomass production

Soil samples were collected from south of Baghdad city surface layer to a depth of 5cm, sample was stored at 4 C° over night until use. 1g soil is diluted in 10ml of sterile distilled water depending on serial dilution method 1 ml of the dilution transferred into potato dextrose agar plates were incubated at 28 C° for 7 days. Also using Potato Dextrose Agar medium for isolation and purification of *M. rouxii* from mixed culture, in sterilized PDA plates until abundant growth for further investigation [7]. Identification of *M. rouxii* depend on microscopic morphology of hyphae and colony features. Biomass production was done according

to [8,9]. Mycelial cells of *M. rouxii* were inoculated in PDB flasks were incubated in growth conditions chosen consistent with prior researches for 96 hrs. at 30 C° in a shaking incubator at 150 rpm [10,11]. Following the incubation time, the fungal biomass was collected by vacuum filtration and washed twice with centrifugation using sterile distilled deionized water at 4,000 rpm/min for 5 minutes to neutrality. The resultant mycelia were then dried to a consistent weight at 40 C° for 24 hrs. the dried mycelial mass was ground in the hood under sterile conditions with a mortar and pestle. Finally, the fungal mycelial mass was powdered and weighted for biomass determination and chitosan extraction.

#### Extraction of fungal chitosan

Powdered biomass of *Mucor rouxii* were grounded and homogenized under sterile conditions in the hood using mortar and pestle. and using the procedure previously described by [11], then subjecting to a 2%(w/v) sodium hydroxide solution at a ratio of 1:30 (w/v) and autoclaved at 121 C°, 15 pounds per square inch for 30 min[11]. The mixture was then cooled then washed with distilled deionized water and centrifugation at (10000 rpm, 15 min, 4 °C) and repeating this process several times until the pH became neutral. Also repeating the base treatment as deacetylation with changing only the concentration to 10% NaOH. then the alkali-insoluble fraction obtained from the deacetylation step was separated, then by using 10% acetic acid with a ratio of 1:40 (w/v) and autoclaved at 121°C, 15 pounds per square inch for 30 min, and centrifuged (10000 rpm, 15 min, 4 °C). The supernatant was alkalized to pH 10 with 4 M NaOH, allowed to stand overnight at 5 °C, then centrifuged for chitosan precipitation at (10000 rpm, 15 min, 4°C). Extracted chitosan was rinsed with distilled deionized water and 95% ethanol (1: 20 w/v) before being dried in a forced air oven at 50°C for 24 hrs [12].

#### Characterization Of Chitosan

##### 1. Chitosan yield

Yield was estimated by the following equation [12].

$$\text{yield of chitosan \%} = \frac{\text{dry weight of chitosan yielded (g)}}{\text{dry weight of fungal biomass (g)}} \times 100\% \quad \dots (1)$$

##### 2. Fourier transform infrared (FTIR) spectroscopy

FTIR analyses were performed with FT-IR spectrophotometer. A pellet of mixed chitosan powder and anhydrous potassium bromide was formed in a mass ratio of 1:100 to make the samples. Analyses were performed at resolutions ranging from 400 to 4000 cm<sup>-1</sup>, with 100 scans averaged at 4 cm<sup>-1</sup> [13].

##### 3. Degree of Deacetylation (DD%)

Determined using FTIR analysis of the produced chitosan and the formula proposed by [13]:

$$DD\% = 100 - \left[ 31.92 \left( \frac{A_{1320}}{A_{1420}} \right) - 12.20 \right]$$

Whereas A1320 absorption of band at 1320 cm<sup>-1</sup> is a distinctive band of the acetylated amide that measures the amount of N-acetylation of chitosan, A1420 absorption of band at 1420 cm<sup>-1</sup> is a peak employed as the reference band.

#### 4. Molecular weight of chitosan

The molecular weight of chitosan was determined by the viscosity of the polymer according to the procedure described by [14].

##### 4.1. Determination of intrinsic viscosity of chitosan

The Ostwald viscometer with capillary (0.5 mm) was used to measure the viscosity. Before the first measurement, the temperature of the water bath was sustained at 25°C and monitored for at least 10 minutes. Then, using a glass pipette, 10 ml of filtered solvent (acetic acid/ sodium acetate) was pipetted into the Ostwald viscometer.

The following viscosities were determined using the relevant formulae for each chitosan concentration: relative viscosity (  $\eta_r$  ), specific viscosity (  $\eta_{sp}$  ), and reduced viscosity (  $\eta_{red}$  ).

$$\eta_r = \frac{t}{t_0} \quad \dots(3)$$

$$\eta_{sp} = \eta_r - 1 \quad \dots(4)$$

$$\eta_{red} = \frac{\eta_{sp}}{c} \quad \dots(5)$$

Where  $t$  is the flow time of chitosan solution (chitosan + solvent system) and  $t_0$  is the flow time of solvent (acetic acid and sodium acetate) in seconds, and  $c$  is the chitosan concentration in g/dl.

After that, an extrapolation plot showing reduced viscosity against chitosan concentration was constructed using a trend line. The intrinsic viscosity was defined as the Y intercept at zero concentration of polymer solution [15].

##### 4.2. Determination of Molecular Weight of Chitosan

Viscometrical data with an Ostwald capillary viscometer were used to determine the viscosity-average molecular weight. Mark-Houwink-Sakurada equation was used to determine this value.

$$[\eta] = KM^\alpha$$

Where  $K = 0.078$  and  $\alpha = 0.76$ , determined in 0.3M acetic acid solution and 0.2M sodium acetate at 25°C, based on a previous study [15].

##### Antimicrobial activity of fungal chitosan

Bacterial inoculum preparation of *Staphylococcus aureus*, *Escherichia coli*, and *Acinetobacter baumannii* Antibiotic susceptibility test of Staphylococcaceae and Enterobacteriaceae using VITEK® 2 System, after identification, bacteria were maintained alive by transferring a single pure isolated colony to brain heart infusion broth medium containing 15% glycerol. It was used to keep bacterial isolates for an extended period of time at a temperature of 0 °C [16].

### Broth Microdilution Assay

A susceptibility panel in 96-well microtiter plates was prepared for the broth microdilution test by pipetting 20  $\mu$ l of chitosan stock solution with the highest concentrations into the first column wells and 160  $\mu$ l of Mueller hinton broth. Then, the first column's two-fold serial dilution chitosan solution is welled into the second-column, and the process is repeated to obtain the final concentrations. Aliquots of 20  $\mu$ l from every bacterial cell suspension were injected into the microtiter plate wells to achieve a final volume of 200  $\mu$ l in each well. The final two wells served as controls, one negative and one positive, respectively. The negative wells were left blank without inoculation, while the positive control of chitosan free solution was inoculated with bacterial suspension and 1% acetic acid solution. The 96 microwell plates were sealed and incubated at 37 °C for 24 hrs [16].

### Determination of Minimum Inhibitory Concentration (MIC) using Resazurin

The MICs for chitosan were determined as the lowest concentration at which no viable cells were found in the wells of 96-microwell plates after 24 hours of incubation. and it's done by aliquots of 10  $\mu$ l resazurin was added to all wells and further incubated for 4 hrs. for the observation of color change. The lowest concentration of no color change from blue to pink (blue resazurin color remained unchanged) was to be scored as the MIC value [17].

### Statistical Analysis

Two-way analysis of variance ANOVA, Least Significant Difference (LSD) and correlation was performed to test whether group variance was significant or not ( $p \leq 0.01$ ) Data were expressed as mean  $\pm$  Standard Deviation (SD) and statistical significance were carried out using SPSS program version 26.

## III. RESULTS

### Identification of *Mucor rouxii*

Depends on fungal colony and aerial hyphae morphology which developed white growth that eventually turned to brownish to dark black patches, which were sporangiophores. Mycelia of the fungal expanded rapidly, with many stolons connecting clusters of unbranched sporangiophores ranging in color from hyaline to slightly gray. Sporangiophores terminate in a huge, cylindrical columella. Sporangiophores feature a single spherical sporangium that is cylindrical, round or conical in shape, white to gray in color, and covered with many angular, sub-globose, and ellipsoidal ridges. Rhizoids were observed adjacent to the as shown in figure (1). These morphological descriptions corresponded to those given by [18].

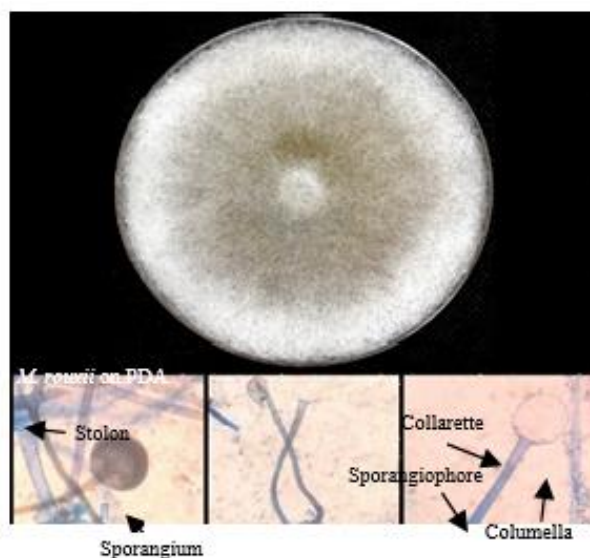


Figure 1. *M. rouxii* in the current study  
Magnification power = 40 X.

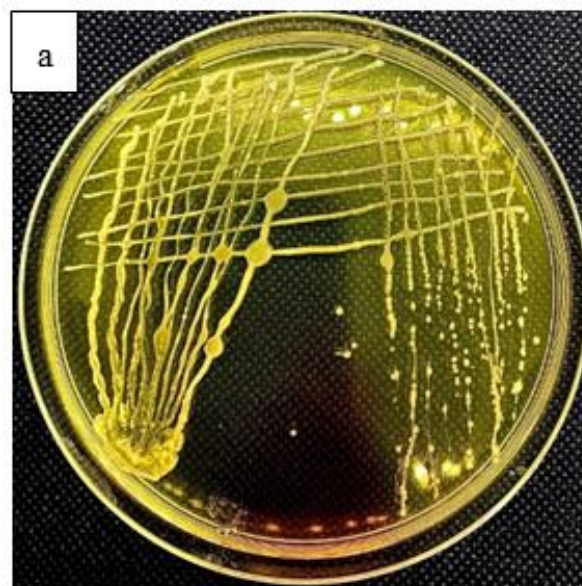
### Microscopic Examination of Bacteria

Microscopical inspection of *P. aeruginosa* isolates using the gram stain revealed cells with gram-negative single rod shapes [19].

In the instance of *S. aureus*, Gram stain revealed cocci that were organized in pairs or clusters and were no spore forming [20].

Microscopy of *E. coli* revealed that it is a gram-negative bacterium that is rod-shaped, aggregates singly or in pairs, and does not produce spores [20].

Whereas *A. baumannii* isolates obtained from MacConkey agar medium were identified using the Gram stain, *A. baumannii* contained gram-negative coccobacilli arranged in a diplococcal pattern [21]. As shown in figure (2).



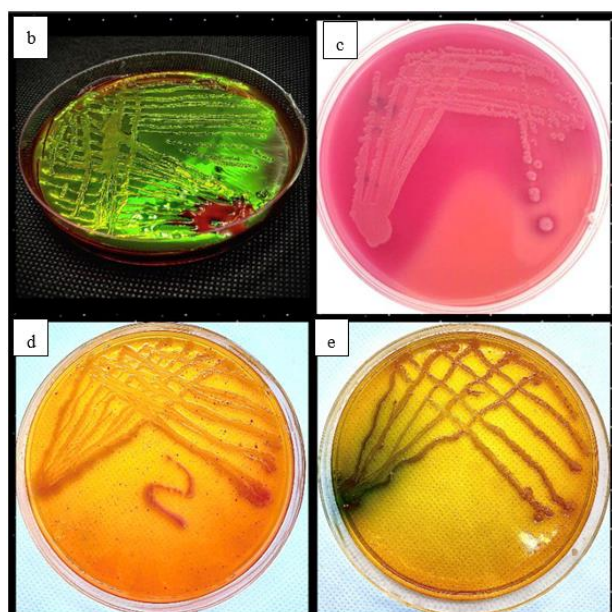


Figure 2: a) *S. aureus* on Mannitol Salt agar, b) *E. coli* on EMB, c) *E. coli* on MacConkey agar, d) *A. baumannii* on MacConkey agar, and e) *P. aeruginosa* on MacConkey agar.

#### Biochemical Examination of Bacteria

A variety of biochemical assays were performed on *P. aeruginosa*, *S. aureus*, *E. coli*, and *A. baumannii* isolates in order to characterize them, the biochemical test results were compared to the bacteria's characteristics as described by [21], the results of which are summarized in (table 1). These results demonstrate that gram negative bacteria were positive for catalase, negative for oxidase with the exception of *P. aeruginosa*, and non-lactose fermenters except for *E. coli*, which appears to be lactose fermenter. while gram positive bacteria *S. aureus*, was positive for catalase and coagulase but negative for oxidase.

Table 1: Gram stain and Biochemical tests of bacteria for the current study.

Biochemical test	Result			
	<i>P. aeruginosa</i>	<i>S. aureus</i>	<i>E. coli</i>	<i>A. baumannii</i>
Gram stain	Gram negative rods	Gram positive cocci	Gram negative rods	Gram negative rods
Catalase test	Positive	Positive	Positive	Positive
Oxidase test	Positive	Negative	Negative	Negative
Lactose fermenting	Negative	N/A	Positive	Negative
Coagulase test	N/A	Positive	N/A	N/A

## IV. DISCUSSION

#### Biomass yield

Mycelial biomass accumulation is an important indicator of growth rate of fungal. Carbohydrate in PDB medium is the main carbon source of heterotrophic microorganism. Carbohydrate absorption capacity represents energy and material metabolism status of fungal [22]. *M. rouxii* was cultivated in Potato dextrose Broth for 96 hrs. at 30°C in a shaking incubator at 150 rpm and 5.5 pH, then the fungal mycelial were dried at 40 °C grounded and weighted. the result of mycelial dry weight in total was 68.8g with a yield of  $1.72 \pm 0.25$  g/500ml. Another study was close to the current results done by [23] who recorded biomass of *M. rouxii* cultivated in PDB using shaking incubator was 0.7g/100ml. Study by<sup>24</sup> recorded that biomass yield was 0.359 g /100ml from cultivation of *Aspergillus ochraceus* in PDB.

#### Chitosan extraction

Chitosan was produced from black bread mold *mucor rouxii* using the classic chemical method. In the current study, alkaline treatment with a dilute sodium hydroxide solution is the most important treatment step because it removes proteins and other cell wall components. After that deacetylation occur by arising NaOH to 10%, next the solid phase corresponds to the insoluble alkaline fraction, which is indicated by the abbreviation AIM (alkaline insoluble material). AIM was formerly separated from chitosan by dissolving it in an acid solution and then separating the resultant material into two components: the acid insoluble chitin component and the soluble chitosan component, which was precipitated with 4M sodium hydroxide [12].

The chitosan yield from *mucor rouxii* was 2.13%. which is higher than [25] who recorded that chitosan yield was 1.9%.

A study done by [26] determined the yield % of chitosan in the dry mass of cicada slough, grasshopper, mealworm, and silkworm chrysalis, was to be 28.2 %, 5.7 %, 2.5 %, and 3.1 %, respectively [27]. reported that *Rhizomucor miehei* and *Mucor racemosus* cultivated in Sabouraud dextrose broth were 13.67%, and 11.72%, respectively [12] reported that under optimum conditions, chitosan yield from *Aspergillus niger* was 7%. Another study by<sup>28</sup> showed the maximum yields of chitosan from *Saccharomyces cerevisiae* using a culture broth containing sodium acetate were  $20.85 \pm 0.35$  mg/g dry biomass.

#### Characterization of chitosan

##### Fourier transform infrared (FTIR) spectroscopy

Infrared spectroscopy is a critical and commonly used diagnostic method for determining the functionality groups and the structural atomic molecules [13]. The infrared spectrum of chitosan obtained from *mucor rouxii* was described and matched to that of standard chitosan using FTIR spectroscopy.

The FTIR spectra of the extracted chitosan's from *M. rouxii* were: a broad band at 3423 and 3446  $\text{cm}^{-1}$ , respectively assigned to hydrogen-bonded O-H stretching vibrations that overlapped with the N-H stretching band, as well as the intramolecular hydrogen bonds and the absorption bands at 2935  $\text{cm}^{-1}$  for the extracted chitosan's showed C-H symmetric stretching vibration in CH3 bonds. The third type of characteristic absorption wavelength for chitosan groups is 1650  $\text{cm}^{-1}$ , which confirms the existence of a C=O group on the bond. (-NHCOCH<sub>3</sub>), the results of the current study were 1647 for the extracted chitosan.

The absorption bands at 1593  $\text{cm}^{-1}$  for the extracted chitosan indicated the presence of a stretching vibration consistent with amide II's N-H bending. The appearance of bands at around 1427, and 1381  $\text{cm}^{-1}$  confirms the CH<sub>2</sub> bending and CH<sub>3</sub> symmetrical deformations, respectively for the extracted chitosan. The bands at 1321  $\text{cm}^{-1}$ , for the extracted chitosan's correspond to C-N stretching in Amide III group.

The absorption band at 1156, 1080  $\text{cm}^{-1}$ , for the extracted chitosan. attributed to asymmetric stretching of the C-O-C bridge. the bands at 1029  $\text{cm}^{-1}$ , respectively for the extracted chitosan correspond to C-O stretching in secondary OH group. Pyranose ring skeletal vibrations were at 889  $\text{cm}^{-1}$  for the extracted chitosan.

This arrangement of absorption bands was identical to that observed in the standard chitosan spectra, particularly at wavenumbers 3394, 2924, 1650, 1560, 1423, 1370, 1251, 1153, 1076, 1026, and 864  $\text{cm}^{-1}$  figure(3) and table (2). except for the band of (C-N) of amide III it maybe overlapped by other bands near it in the extracted chitosan. Based on an infrared spectrum study in comparison to standard chitosan. The existence of the primary spectrum in particular wavelength areas suggests the presence of a significant functional group, indicating that the chemically extracted molecule is chitosan. Also, the result of the current study was in agreement with previous studies [29].

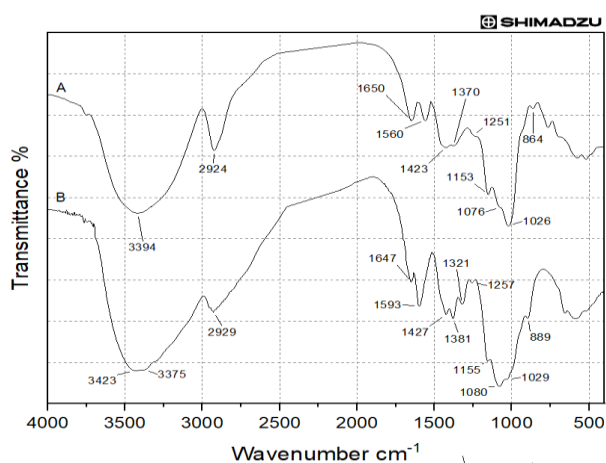


Figure 3: FTIR spectra and absorption bands of chitosan in the current study. A) chitosan standard, B) chitosan from *M. rouxii*.

Table 2. FTIR absorption band and assignment for chitosan in the current

NO.	Assignment	Standard chitosan	<i>M. rouxii</i>
		Wavenumber $\text{cm}^{-1}$	
1.	(NH <sub>2</sub> ) association in primary amines overlapping with (OH) association in pyranose ring	3394	3423
2.	(C-H) stretching band	2924	2935
3.	(C=O) in NHCOCH <sub>3</sub> Amide I band	1650	1647
4.	(NH <sub>2</sub> ) in NHCOCH <sub>3</sub> Amide II band	1560	1593
5.	(CH <sub>2</sub> ) in CH <sub>2</sub> OH group	1423	1427
6.	(CH <sub>3</sub> ) in NHCOCH <sub>3</sub> Amide III band	1370	1381
7.	(C-N) of amide III	Not found	1321
8.	Complex vibrations of NHCO group (Amide III band)	1251	1257
9.	(C-O-C) (glycosidic linkage)	1153	1156
10.	(C-O-C) (glycosidic linkage)	1076	1080
11.	(C-O) in Pyranose ring	1026	1029
12.	Pyranose ring skeletal	864	889

#### Degree of deacetylation of chitosan

The characteristic that strengthens and confirmed the product in the current study was chitosan is characterized by the appearance of wave absorption bands compared with standard chitosan. Additionally, the loss of the methyl (CH<sub>3</sub>) group linked to the amide may be seen in the reduction of absorption at wavenumbers 2935  $\text{cm}^{-1}$ . And the loss of group COO in amide is determined by the absence of absorption bands at 1647  $\text{cm}^{-1}$  [30].

FTIR spectroscopy was used to analyze chitosan derived from the fungal biomass of *M. rouxii*. The data acquired enabled recognition of the extracted chitosan as well as determination of the degree of deacetylation, a critical characteristic affecting the biopolymer's physiochemical and biological characteristics.

The degree of deacetylation of chitosan extracted from *M. rouxii* was 82.22%. At 1647, 1593  $\text{cm}^{-1}$ , the amide I and amine bands of chitosan extracted

from *M. rouxii* were detected. The bands at  $1593\text{ cm}^{-1}$  of the extracted chitosan were rather intense when compared to the standard chitosan, indicating sustained deacetylation in the fungal chitosan extracted in the current study, as seen in Figure(3).

Deacetylation decreases the intensity of the amide I band while increases the intensity of the amide II band, suggesting the presence of  $\text{NH}_2$  groups [311]. When the spectrum between  $1500$  and  $1700\text{ cm}^{-1}$  is narrowed, an intensification occurs, suggesting the existence of effective deacetylation. chitosan from *M. rouxii* which has small absorption intensity at  $1647\text{ cm}^{-1}$  and medium intensity at  $1593\text{ cm}^{-1}$ . As a result of protonation of the  $-\text{NH}_2$  function on the C2 position of the repeating unit D-glucosamine, the degree of deacetylation rises as the number of acetyl groups decreases, producing high-quality chitosan [27].

Chitin and chitosan are produced in relatively significant amounts by zygomycetes and basidiomycetes, it found in the inner layer of the cell wall adjacent to the plasma membrane and is responsible for the cell wall's structure, strength, and integrity [32]. Water, proteins, and a NaOH-insoluble fraction including chitin as well as a little amount of chitosan, are the primary components of mycelium [33]. So, using deproteinization step to discard cell wall component as alkali soluble material and yield chitin and chitosan as alkali insoluble material.

In the current study deacetylation of chitosan were carried out by NaOH 10% of AIM, and due to the fact that deacetylation of chitosan needed the nucleophilic breakage of the C-N bond, a particular activation energy was required, which could be provided by the autoclave's high temperature and pressure. Then treating the product by acetic acid 10% to solubilize and separate chitosan from chitin which is insoluble in acids<sup>11</sup>. The degree of deacetylation depends on method of extraction method, incubation time and temperature, and source. A study done by [34] determined the DD of chitosan from shrimp waste was 88%. another study done by<sup>56</sup> who recorded DD of chitosan from *Penicillium chrysogenum* was 82.4%.

The results of the current study were higher than the results done by [35]who recorded the DD of *M. rouxii* CTS1551n was 77.3%.

#### Chitosan's molecular weight

Molecular weight of chitosan extracted from *M. rouxiia* y using the Mark-Houwink-Sakurada equation was 63.67 kDa. The curves plotting of reduced viscosity of chitosan extracted from *M. rouxiia* persus chitosan concentrations as shown in Figure (4) demonstrate that all experimental points are fairly well matched along straight lines ( $R^2=0.93$ ). The viscosity measurements on *M. rouxiia* extracted chitosan enabled the estimation of the intrinsic viscosity and viscosity average molecular weights.

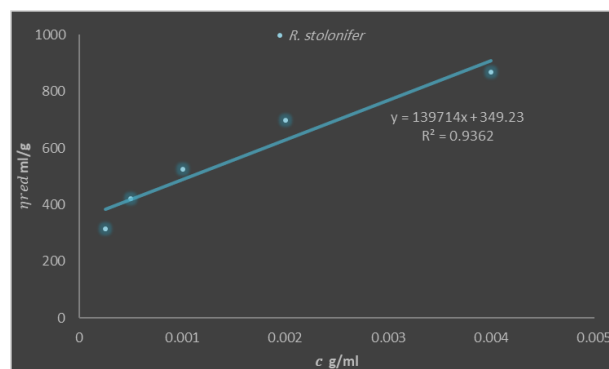


Figure 4: Curves of reduced viscosity ( $\eta_{red}$ ) against concentrations of chitosan extracted from *M. rouxii*

When the concentration approaches zero, the polymer molecules become dissociated and interact exclusively with the solvent molecules. However, because this condition is seldom achievable in actuality, it is necessary to address minute polymer interactions, this scattered viscosity data may imply that the produced chitosan is polydisperse in nature [36].

As a result of the interaction of the acid carboxyl groups with the hydroxyl groups of chitosan, glycosidic linkages are broken, resulting in the breakdown of chitosan molecules [37].

Because chitosan is insoluble in water, the production of complex ions from amine on chitosan and acetic acid improves solubility and works in a way as catalytic. The entangle of the nucleophilic amine with the glycosidic bond occurs at high reaction temperatures. Due to an increased mobility generated by the autoclave's high temperature, the probability of encountering and entangling the protonated amine with the glycosidic bond increased. Following the initial phase of encounter and entanglement, the next stage is protonation of the glycosidic oxygen atom, which may be accomplished through stereo configuration inference. When the exocyclic O-5 to C-1 link is heterolyzed to generate a cyclic oxocarbenium ion, which most likely occurs in the half chair conformation with C-2, C-1, O-5, and C-5 in a plane, the stereo configuration is smaller and hence desirable [37]. The last step is the reaction with water, which produces the reducing sugar. As a result, chitosan acid depolymerizes. However, in this work, the DD of the extracted chitosan was 82.22%, therefore the difference in hydrolysis rate between the glycosidic linkage following an N- deacetylated unit and that following a N-acetylated unit was only of small relevance.

Molecular weight of *M. rouxii* was 63.67kDa. which was deemed to be rather low. It has been found that chitosan produced from fungal mycelia has a low to medium molecular weight (10–120 kDa), but chitosan derived from crustaceans has a high molecular weight about  $1.510^3$  kDa [38].

**Antibacterial activity of chitosan**

The antibacterial activity of isolated chitosan from *M. rouxii* towards tested bacterial strains Table (3) is summarized in Table (4). After treating it with chitosan extracted from *M. rouxii*, all of the investigated

bacterial strains shown a range of sensitivities. As indicated in figure (4), the most resistant bacteria that required the highest MIC values were *S. aureus*, whereas the most sensitive strains were *A. baumannii* and *E. coli*.

**Table 3: Basic features of bacterial strains used in the current study.**

microbial strain	gram stain	origin	growth media	Growth temperature
<i>A. baumannii</i>	G-	clinical	Nutrient agar	37°C
<i>E. coli</i>	G-	clinical	Nutrient agar	37°C
<i>P. aeruginosa</i>	G-	clinical	Nutrient agar	37°C
<i>S. aureus</i>	G+	clinical	Nutrient agar	37°C

**Table 4: Minimal inhibitory concentrations (µg/ml) of chitosan from *M. rouxii* types against examined bacterial strains**

Descriptive Statistics		
Bacteria	Mean±SD	N
<i>A. baumannii</i>	250 ±0.0 <sup>c</sup>	3
<i>E. coli</i>	250 ±0.0 <sup>c</sup>	3
<i>P. aeruginosa</i>	333.33 ± 144.33 <sup>b</sup>	3
<i>S. aureus</i>	500 ±0.0 <sup>a</sup>	3

The different letter = high significant difference at  $p \leq 0.01$

The similar letter = non-significant at  $p \geq 0.01$

treated with the resazurin dye. Row G verifies that there was no contamination during the plate preparation process. Row H, a positive control, demonstrated a change in the color of resazurin from its native state (blue) to its reduced state (pink), showing that the 1% acetic acid solution promotes bacteria growth in another word acetic acid didn't show effect on bacterial growth. The highest concentration inserted onto the plate is 1000 µg/ml, while the lowest concentration obtained after twofold serial dilution is 31.25 µg/ml.

The MIC values of chitosan concentrations in the wells were between 250–500 µg/ml depends on the different bacteria and the sources of extracted chitosan as shown in figure(4).

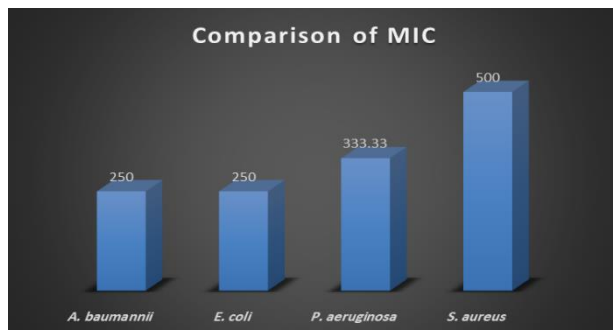


**Figure 4: comparison of MIC (µg/ml) between the chitosan extracted from *M. rouxii***

The present work employed resazurin to determine the MIC of chitosan, as seen in figure(5), and table (5). After a period of incubation, the bacteria were

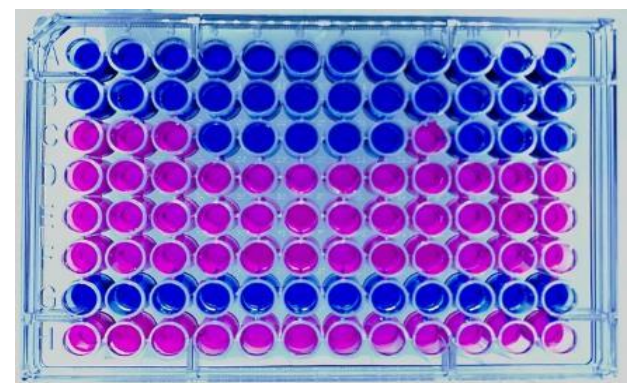


**Figure 5: Resazurin color change as identification of MIC of bacteria of *M. rouxii* chitosan, whereas blue color represents absent growth of bacteria, while pink color represents growth of bacteria.**

**Table 5: Schematic representation of the 96-well plate and the MIC of chitosan extracted from *M. rouxii*.**

Bacteria	<i>S. aureus</i>			<i>E. coli</i>			<i>P. aeruginosa</i>			<i>A. baumannii</i>			
	1	2	3	4	5	6	7	8	9	10	11	12	
Concentration µg/ml													
A	1000	+	+	+	+	+	+	+	+	+	+	+	
B	500	MIC			+	+	+	+	+	MIC			
C	250	-	-	-	MIC			MIC			-	MIC	
D	125	-	-	-	-	-	-	-	-	-	-	-	
E	62.5	-	-	-	-	-	-	-	-	-	-	-	
F	31.25	-	-	-	-	-	-	-	-	-	-	-	
G	-V. Control	+	+	+	+	+	+	+	+	+	+	+	
H	+V. Control	-	-	-	-	-	-	-	-	-	-	-	

(-) bacterial growth, (+) absent bacterial growth

The availability chitosan in a variety of molecular weights, deacetylation degrees, and modified forms for a variety of applications. As a result, biomedical applications require the antibacterial capabilities of a certain chitosan and its modified form. In our daily lives, *P. aeruginosa*, *E. coli*, *A. baumannii*, *S. aureus*, and a variety of other important bacterial pathogens are frequently responsible for nosocomial infections. These pathogens are vulnerable to developing resistance to a range of antibiotics used in preventative treatment. As a consequence, it was determined that resistance developed as a result of multiple antibiotics' ineffectiveness [39]. Thus, the two primary goals in the development of new antimicrobial drugs are to improve the efficacy of antibiotics and reduce their toxicity.

In the current study, significant MIC of the tested bacteria by the extracted chitosan was observed; however, the MIC were different with the difference of chitosan source, molecular weight, and degree of deacetylation.[40] The particular processes behind chitosan's and its derivatives' antibacterial action are not fully defined, while numerous processes have been postulated. Several hypothesized pathways all require some form of cell membrane damage or interactions. The most suited interaction is between positively charged chitosan molecules and negatively charged microbial cell membranes. In this concept, the contact is mediated by electrostatic interactions between the protonated amino groups and the negative residues. Probably through contesting for electronegative regions on the membrane surface with  $Ca^{2+}$  [41].

In the current study, the results of MIC of the extracted chitosan from *M. rouxii* in the case of gram-negative bacteria were more effective than gram-positive bacteria. In terms of surface polarity, the outer membrane of gram-negative bacteria is mostly formed of lipopolysaccharides containing phosphate and pyrophosphate groups, which provide the surface a higher density of negative charges than gram-positive bacteria which its membrane composed by peptidoglycan associated to polysaccharides and teichoic acids [42].

The results of the current study was lower than a study done by<sup>43</sup> recorded the MIC of the extracted from *P. ostreatus* towards *E.coli* was 0.65 mg/ml. Another study done by<sup>44</sup> recorded MIC of 78- 625  $\mu$ g/ml for the bacteria in his study.

## V. CONCLUSIONS

Chitosan was effectively produced through the cultivation of *M. rouxii* on PDB as carbon source. This study concluded that the cultivation of *M. rouxii* extract has high potential for chitosan production as an eco-friendly method. Mod of chitosan action is attachment to the bacterial cell wall and the most resist bacteria was *S. aureus*.

## ACKNOWLEDGMENTS

The authors extend their gratitude to Biology Department College of Sciences at Mustansiriyah University for their financial support.

## REFERENCES

- [1] Abdou ES, Nagy KSA, Elsabee MZ. Extraction and characterization of chitin and chitosan from local sources. *Bioresour Technol.* 2008;99(5):1359–67.
- [2] Badawy MEI, Rabea EI. A biopolymer chitosan and its derivatives as promising antimicrobial agents against plant pathogens and their applications in crop protection. *Int J Carbohydr Chem.* 2011;2011.
- [3] Abdelrazek EM, Elashmawi IS, Labeeb S. Chitosan filler effects on the experimental characterization, spectroscopic investigation and thermal studies of PVA/PVP blend films. *Phys B Condens Matter.* 2010;405(8):2021–7.
- [4] Tajik H, Moradi M, Rohani SMR, Erfani AM, Jalali FSS. Preparation of chitosan from brine shrimp (*Artemia urmiana*) cyst shells and effects of different chemical processing sequences on the physicochemical and functional properties of the product. *Molecules.* 2008;13(6):1263–74.
- [5] Tayel AA, Moussa S, Wael F, Knittel D, Opwis K, Schollmeyer E. Anticandidal action of fungal chitosan against *Candida albicans*. *Int J Biol Macromol.* 2010;47(4):454–7.
- [6] Kannan M, Nesakumari M, Rajarathinam K, Singh A. Production and characterization of mushroom chitosan under solid-state fermentation conditions. *Adv Biol Res.* 2010;4(1):10–3.
- [7] Solairaj D, Legrand NNG, Yang Q, Zhang H. Isolation of pathogenic fungi causing postharvest decay in table grapes and in vivo biocontrol activity of selected yeasts against them. *Physiol Mol Plant Pathol.* 2020;110:101478.
- [8] Lee J-H, Cho S-M, Ko K-S, Yoo I-D. Effect of cultural conditions on polysaccharide production and its monosaccharide composition in *Phellinus linteus* L13202. *Korean J Mycol.* 1995;23(4):325–31.
- [9] VALENZUELA-COBOS JD, GRIJALVA-ENDARA ANA. Sorption of Zinc by exopolysaccharides produced by liquid media of phytopathogenic fungi. 2021;
- [10] Berger LRR, Stamford TCM, Stamford-Arnaud TM, De Alcântara SRC, Da Silva AC, Da Silva AM, et al. Green conversion of agroindustrial wastes into chitin and chitosan by *Rhizopus arrhizus* and *Cunninghamella elegans* strains. *Int J Mol Sci.* 2014;15(5):9082–102.
- [11] Ramos Berger LR, Montenegro Stamford TC, de Oliveira KÁR, de Miranda Pereira Pessoa A, de Lima MAB, Estevez Pintado MM, et al. Chitosan produced from Mucorales fungi using agroindustrial by-products and its efficacy to inhibit *Colletotrichum* species. *Int J Biol Macromol [Internet].* 2018;108:635–41. Available



from: <http://dx.doi.org/10.1016/j.ijbiomac.2017.11.178>

- [12] Abdel-Gawad KM, Hifney AF, Fawzy MA, Gomaa M. Technology optimization of chitosan production from *Aspergillus niger* biomass and its functional activities. *Food Hydrocoll.* 2017;63:593–601.
- [13] Eddy M, Tbib B, Khalil E-H. A comparison of chitosan properties after extraction from shrimp shells by diluted and concentrated acids. *Heliyon.* 2020;6(2):e03486.
- [14] Malm M, Liceaga AM. Physicochemical Properties of Chitosan from Two Commonly Reared Edible Cricket Species, and Its Application as a Hypolipidemic and Antimicrobial Agent. *Polysaccharides.* 2021;2(2):339–53.
- [15] Kabir MT, Kabir MS, Miah AB, Sarker MAK, Pramanik MK. Physicochemical Properties of Chitosan Extracted from *Pleurotus ostreatus* and Improvement of its Antibacterial Activity by Gamma Radiation. *Bangladesh J Microbiol.* 2020;37(2):52–5.
- [16] Vandepitte J, Verhaegen J, Engbaek K, Piot P, Heuck CC, Rohner P, et al. Basic laboratory procedures in clinical bacteriology. World Health Organization; 2003.
- [17] Kavuo S, Namboko JK, Bukusuba S. Antimicrobial interactions between the phytoextracts of. 2021;
- [18] Shipper MAA. A revision of the genus *Rhizopus* I. The *mucor rouxii*-group and *Rhizopus oryzae*. *Stud Mycol.* 1984;25:1–19.
- [19] Bakheet A, Torra D. Detection of *Pseudomonas aeruginosa* in Dead Chicken Embryo with Reference to Pathological Changes and Virulence Genes. *Alexandria J Vet Sci.* 2020;65(1):81.
- [20] Tandyono V. Microbiological Aspect Of Staphylococcal Infection In Severe Degree Of Burns. *J Widya Med [Internet].* 2021 Oct 31 [cited 2022 Jan 28];7(2):127–40. Available from: <http://jurnal.wima.ac.id/index.php/JWM/article/view/3307>
- [21] Al-Daraghi WAH, Al-Taliby SA. Study the Incidence of *Acinetobacter Baumannii* as a Nosocomial Pathogen. *Indian J Public Heal Res Dev.* 2019;10(10).
- [22] Wang Y, Zhang X, ZHOU J-Y, LI X-C, Min J, LAI T-F, et al. Inhibitory Effects of Five Antifungal Substances on Development of Postharvest Pathogen *Rhizopus oryzae*. *J Agric Biotechnol.* 2015;23(1):107–17.
- [23] Valenzuela-Cobos JD, Grijalva A, Marcillo R, Garcés F. Production of exopolysaccharides of *Colletotrichum gloeosporioides* and *mucor rouxii* to absorb lead in the sediment of aquaculture pool. *Egypt J Aquat Biol Fish.* 2020;24(7-Special issue):41–9.
- [24] Rahman RU, Mathur G. Effect of Different Media on Growth Kinetics Parameters of *Aspergillus ochraceus*: an Approach Towards Production of Fungal Biomass. *Curr Trends Biotechnol Pharm.* 2021;15(6):1–3.
- [25] Hu KJ, Hu JL, Ho KP, Yeung KW. Screening of

fungi for chitosan producers, and copper adsorption capacity of fungal chitosan and chitosanaceous materials. *Carbohydr Polym.* 2004;58(1):45–52.

- [26] Luo Q, Wang Y, Han Q, Ji L, Zhang H, Fei Z, et al. Comparison of the physicochemical, rheological, and morphologic properties of chitosan from four insects. *Carbohydr Polym [Internet].* 2019;209(January):266–75. Available from: <https://doi.org/10.1016/j.carbpol.2019.01.030>
- [27] Tajdini F, Amini MA, Nafissi-Varcheh N, Faramarzi MA. Production, physicochemical and antimicrobial properties of fungal chitosan from *Rhizomucor miehei* and *Mucor racemosus*. *Int J Biol Macromol.* 2010;47(2):180–3.
- [28] Afroz MM, Kashem MNH, Piash KMPS, Islam N. *Saccharomyces Cerevisiae* as an Untapped Source of Fungal Chitosan for Antimicrobial Action. *Appl Biochem Biotechnol.* 2021;193(11):3765–86.
- [29] Mauricio-Sánchez RA, Salazar R, Luna-Bárceñas JG, Mendoza-Galván A. FTIR spectroscopy studies on the spontaneous neutralization of chitosan acetate films by moisture conditioning. *Vib Spectrosc [Internet].* 2018;94:1–6. Available from: <http://dx.doi.org/10.1016/j.vibspec.2017.10.005>
- [30] Dompeipen EJ. Isolasi dan identifikasi kitin dan kitosan dari kulit udang Windu (*Penaeus monodon*) dengan spektroskopi inframerah. *Maj Biam.* 2017;13(1):31–41.
- [31] de Souza AF, Galindo HM, de Lima MAB, Ribeaux DR, Rodríguez DM, da Silva Andrade RF, et al. Biotechnological strategies for chitosan production by mucoralean strains and dimorphism using renewable substrates. *Int J Mol Sci.* 2020;21(12):4286.
- [32] Brown HE, Esher SK, Alspaugh JA. Chitin: A “hidden figure” in the fungal cell wall. *Curr Top Microbiol Immunol.* 2020;425:83–111.
- [33] Di Mario F, Rapanà P, Tomati U, Galli E. Chitin and chitosan from Basidiomycetes. *Int J Biol Macromol.* 2008;43(1):8–12.
- [34] Jantzen da Silva Lucas A, Quadro Oreste E, Leão Gouveia Costa H, Martín López H, Dias Medeiros Saad C, Prentice C. Extraction, physicochemical characterization, and morphological properties of chitin and chitosan from cuticles of edible insects. *Food Chem [Internet].* 2021;343:128550. Available from: <https://doi.org/10.1016/j.foodchem.2020.128550>
- [35] Cardoso DH, Da Conceição TF, Giachini AJ, Rossi MJ. Chitosans from *mucor rouxii* (strain CBMAI 1551): Characterization and Dense Film Formation. *J Adv Biotechnol.* 2017;6(3):924–31.
- [36] Taghizadeh MT, Abdollahi R. Sonolytic, sonocatalytic and sonophotocatalytic degradation of chitosan in the presence of TiO<sub>2</sub> nanoparticles. *Ultrason Sonochem.* 2011;18(1):149–57.
- [37] Einbu A, Grasdalen H, Vårum KM. Kinetics of hydrolysis of chitin/chitosan oligomers in concentrated hydrochloric acid. *Carbohydr Res.* 2007;342(8):1055–62.

- [38] Nwe N, Furuike T, Tamura H. Production of fungal chitosan by enzymatic method and applications in plant tissue culture and tissue engineering: 11 years of our progress, present situation and future prospects. *Biopolymers*. 2010;7(135):e162.
- [39] Khan J, Tarar SM, Gul I, Nawaz U, Arshad M. Challenges of antibiotic resistance biofilms and potential combating strategies: a review. *3 Biotech*. 2021;11(4):1–15.
- [40] Kipkoech C, Kinyuru JN, Imathiu S, Meyer-Rochow VB, Roos N. In vitro study of cricket chitosan's potential as a prebiotic and a promoter of probiotic microorganisms to control pathogenic bacteria in the human gut. *Foods*. 2021;10(10):2310.
- [41] Fuster MG, Montalbán MG, Carissimi G, Lima B, Feresin GE, Cano M, et al. Antibacterial effect of chitosan–gold nanoparticles and computational modeling of the interaction between chitosan and a lipid bilayer model. *Nanomaterials*. 2020;10(12):2340.
- [42] Yeh V, Bonev BB. Solid-state NMR and dynamic nuclear polarization studies of molecular interactions in membranes. *Solid State NMR*. 2020;1–8.
- [43] Ban Z, Horev B, Rutenberg R, Danay O, Bilbao C, McHugh T, et al. Efficient production of fungal chitosan utilizing an advanced freeze-thawing method; quality and activity studies. *Food Hydrocoll* [Internet]. 2018;81:380–8. Available from: <https://doi.org/10.1016/j.foodhyd.2018.03.010>
- [44] Vilar Junior JC, Ribeaux DR, Alves Da Silva CA, De Campos-Takaki GM. Physicochemical and Antibacterial Properties of Chitosan Extracted from Waste Shrimp Shells. *Int J Microbiol*. 2016.